Asian Journal of Green Chemistry 3 (2019) 366-381

Asian Journal of Green Chemistry

Journal homepage: www.ajgreenchem.com

Orginal Research Article

Green oxidation reactions by graphene oxide-based catalyst with aqueous hydrogen peroxide

Mehrnaz Alem[a], Shahnaz Kazemi[b,*], Abbas Teimouri[a,*], Hossein Salavati[a]

[a] *Chemistry Department, Payame Noor University, 19395-3697, Tehran, Iran*

[b] *Department of Chemistry, Faculty of Science, University of Birjand, P. O. Box 97175-615, Birjand, Iran*

ARTICLE INFORMATION

Received: 17 August 2018
Received in revised: 25 September 2018
Accepted: 25 September 2018
Available online: 28 December 2018

DOI: 10.22034/ajgc.2018.144166.1097

KEYWORDS

Catalytic
Graphene oxide
Green oxidation
Nanocomposite polyethylene glycol

ABSTRACT

This study reports the synthesis, characterization and catalytic properties of a novel supported catalyst on the basis of nickel acetate hydrate (NiOAC) immobilized on graphene oxide (GO) and modified by polyethylene glycol (PEG). The catalyst was characterized by scanning electron microscopy (FESEM), X-ray diffraction spectroscopy (XRD), furrier transforms infrared spectroscopy (FT-IR) and diffuse reluctance spectroscopy (DRS). It showed a high activity in the green oxidation of thioanisole as a model substrate to sulfoxide product at ambient temperature and presurre. To establish the general applicability of the process, various sulfides were subjected to the oxidation system using the synthesized catalyst. The reactivities of the sulfur compounds were influenced by two main factors, i.e., the electron density on the S atom and the steric hindrance of the sulfur compound. In addition, ethanol was selected as a green solvent for this procedure. The effects of the main process variables including H_2O_2 amount (mmol), reaction time (min) and catalyst amount (mg) were analyzed by response surface methodology (RSM) based on the central composite design (CCD). The optimal condition for conversion of thioanisole was found to be O/S ratio 3.4, reaction time 31 min for 21 mg of the catalyst amount.

Graphical Abstract

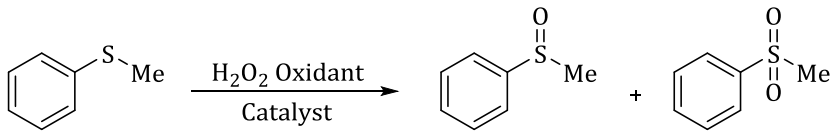

Corresponding author, email: s_kazemi@yahoo.com (Sh. Kazemi); a_teimouri@pnu.ac.ir (A. Teimouri).
Tel.: +9831 33521804; Fax: +9831 33521802.

Introduction

Graphene oxide (GO) with a layered structure is characterized by functional groups such as carboxyl, hydroxyl and epoxide on the surface. It has unique properties such as exceptional thermal properties, strong mechanical strength, high ratio of surface area (2630 m^2/g), etc, [1, 2]. Nanosheets of GO are decorated mostly with functional groups like as epoxide, carboxylic and hydroxyl groups. They possess hydrophilic properties because of the wide range of functional groups which contain oxygen on the surface of GO layers [3, 4]. GO is synthesized through oxidative processing of graphite using one of the principle methods improved by Hummers, Brodie or Staudenmeir. Functionalization of GO can change the mechanical, electrical, thermal and electrical conducting properties of GO; moreover, sulfated graphene was also tested as a catalyst for the oxidation of sulfur-containing compounds [5–14].

PEG can be used as active sites because similar to crown ethers, the polyethylene oxide chains can form stable complexes with metal cations. In order to maintain electro-neutrality, these PEG–metal cation complexes must bring an equivalent anion into the organic phase, and make the anion accessible for reaction with organic reactants. Many factors such as chain end effects, PEG molecular weight, and the nature of associated cations and anions affect phase-catalytic activity [15–21].

Thereupon, the main aim of the present study is to consider a novel system for catalytic and photocatalytic properties by using nickel acetate, immobilized over graphene oxide modified with polyethylene glycol as a natural molecule. The advantage of this catalyst is that we combine the high surface area of the graphene oxide support for the immobilization of the catalytic active metal ions as a heterogenous catalysts with the polyethylene glycol as a carrier of functional and oxygen groups in order to be linked to metal ions; thus creating the active sites. The synthesized catalyst was considered for catalytic oxidation of thioanisole at an ambient pressure and temperature. Accordingly, it showed high catalytic activity and good selectivity to produce sulfoxide from thioanisole with two components, GO and PEG, as environment-friendly and nickel acetate because of having vacant d orbitals for exciting the electron for electron-transfer reactions.

Experimental

Materials and methods

Solvents, chemicals and reagents were obtained from Merck, Fluka or Aldrich Chemical Companies. These samples were ground into a fine powder for characterization. FT-IR spectra were obtained, as potassium bromide pellets, in the range of 400-4000 cm^{-1} with a Nicollet-Impact 400D instrument. Scanning electron microscopy (SEM) of the catalysts and supports were taken using SEM

Philips XL 30 instrument. Diffuse reflactant spectroscopy (DRS) Uv were recorded on a 160 Shimadzu spectrophotometer, and X-ray diffraction (XRD) patterns were recorded with a Philips X-ray diffractometer (Model PW1840). Mass spectrum was also recorded by the GSMS-QP 5050 Shimadzu.

Preparation of graphene oxide (Denoted as GO)

For the improved method, a 9:1 mixture of the concentrated H_2SO_4/H_3PO_4 (360:40 mL) was added to a mixture of $KMnO_4$ (18.0 g, 6 wt equiv) and graphite flakes (3 g, 1 wt equiv) producing a slight exotherm to 35-40 °C. Then, the reaction was heated to 50 °C and was stirred for 12 h. Afterwards, it was cooled to rt and was poured onto ice (400 mL) with 30% H_2O_2 (3 mL). For workup, the mixture was sifted through a metal U.S. Standard testing sieve (W.S. Tyler, 300 m), and then it was filtered through polyester fiber (Carpenter Co.). The filtrate was centrifuged (4000 rpm for 4 h), and the supernatant was decanted away. Then, the remaining solid material was washed with 200 mL of water, 200 mL of 30% HCl, and 200 mL of ethanol in succession. For each wash, the mixture was sifted through the U.S. Standard testing sieve, and then it was filtered through the polyester fiber with the filtrate being centrifuged (4000 rpm for 4 h) and the supernatant being decanted away. After this extended, multiple-wash process, the remaining material was coagulated with 200 mL of ether, and the resulting suspension was filtered through a PTFE membrane with a 0.45 pore size. The solid which was obtained on the filter was vacuum-dried overnight at room temperature, and, consequently, 5.8 g of the product was obtained [22]. The resultant GO has been illustrated in Scheme 1.

Preparation of polyethylene glycol-grafted graphene oxide (Denoted as PEG-GO)

The PEG-modified GO polymeric nanocomposite was prepared by a covalent bond between a polymeric chain of polyethylene glycol and GO, called PEGylation. 0.05 g graphene oxide was dissolved in the minimum possible amount of deionized distilled water and then it was exposed to ultrasonic bath for 5 min. After the solution was removed from the ultrasonic bath, 2 mL of the solution was added to 1 g polyethylene glycol 600, and the mixture was stirred under 300 rpm for 24 h at 25 °C. After some time, the obtained GO was completely dissolved in the hydrophilic polymer. The structure of the resultant composite has been illustrated in Scheme 2 [23].

Preparation of supported catalyst with nickel acetate salt (NiOAC@PEG-GO)

The supported catalyst was synthesized using ultrasonic irradiation method. In this way, 0.1 g PEG-GO was dispersed in ethanol under ultrasonic irradiation for 30 min (Solution 1). Afterwards, the solution of nickel acetate was prepared in ethanol by dispersing 0.05 g simple nickel salt (Solution

2), then solution 2 was added to solution 1 under ultrasonic irradiation for 30 min. This mixture was stirred for 12 h at 60 °C under magnetic stirring prior to being centrifuged and dried in air. The proposed structure of the supported catalyst has been shown in Scheme 3.

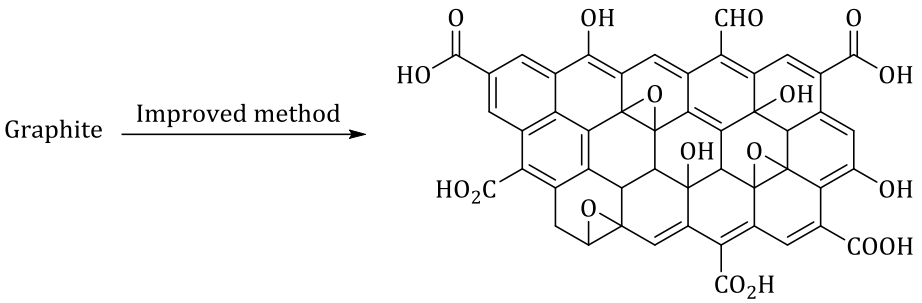

Scheme 1. Structure of synthesized graphene oxide

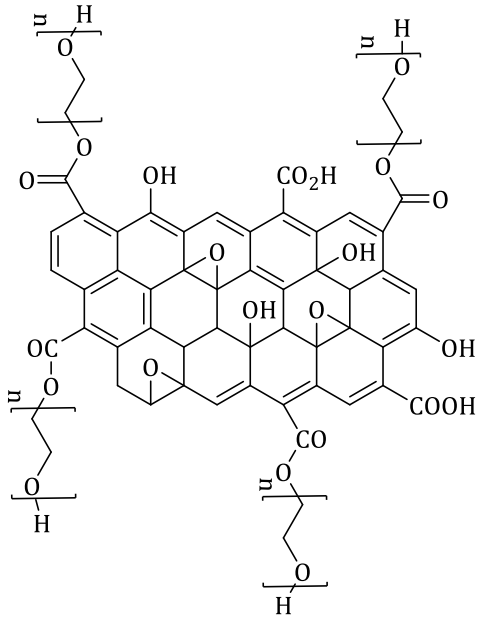

Scheme 2. Structure of synthesized PEG grafted graphene oxide

Results and discussion

Sample characterization

FT-IR spectra are vital tools to characterize both covalent and non-covalent functionalizations of GO. Figure 1 illustrates the FT-IR spectra of the prepared materials, and the following functional groups were identified in all samples: (1720-1740 cm^{-1}) subjected to C=O stretching vibration, (3300-3400 cm^{-1}) related to O–H stretching vibrations, characteristics band for C=C from unoxidized sp^2 C–C bonds appeared in (1590-1628 cm^{-1}), and C–O vibrations appeared at 1228 cm^{-1} and for epoxide

groups at (849, 1048 cm^{-1}) ranges. A band at 1114 cm^{-1} corresponds to the stretching vibration of C–C–O group, a characteristic peak for polyethylene glycol backbone (As illustrated in Figure 1**c**). As shown in Figure 1**a**, the pristine graphite typifies the characteristic band at 3430 cm^{-1} for O–H stretching and at 1610 cm^{-1} for skeletal vibrations from graphitic domains of adsorbed water and aromatic domain (C=C), respectively. Some new peaks at 1726 cm^{-1} for C–O stretching appeared for graphene oxide, 3447 cm^{-1} for O–H stretching, and 1048 cm^{-1} and for C–O stretching. The C–C aromatic peak shows characteristic peak at 1621 cm^{-1} GO because of the presence of some functional groups which withdraw electrons and contain oxygen [22]. Regarding the functionalization of GO with PEG, the -OH stretching peaks (3447 cm^{-1}) of GO are shifted to lower energy vibration at 3443 cm^{-1} for GO-PEG nanocomposite (with 3 wt% GO) indicating the H-bonding interactions between PEG and GO sheets. The 1726 cm^{-1} peak of C–O group shows a shift to 1649 cm^{-1}, and the epoxide stretching vibration of GO at 1048 cm^{-1} has shifted to 1114 cm^{-1} suggesting H-bonding between PEG and epoxy group of GO. The increased frequency of vibration is because of the ring structure of H-bonded epoxy group of GO in the GO-PEG nanocomposites [23]. After the immobilization of acetate nickel on PEG-GO, the broad new peak appearing at 1557 cm^{-1} was related to acetate group confirming that the simple salt of nickel was supported on PEG (As illustrated in Figure 3**d**). The peak related to Ni–O bond was observed below 1000 cm^{-1} ranges.

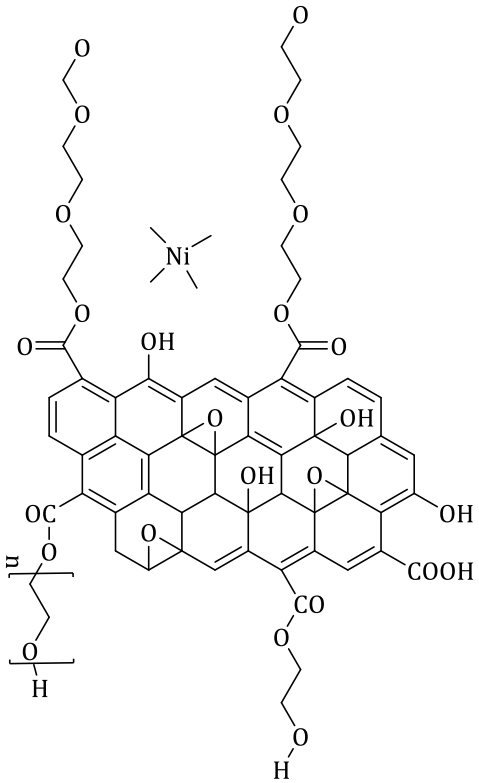

Scheme 3. Proposed scheme for the structure of supported catalyst

Diffuse reflectance (DR) Uv spectra of GO and NiOAC@ PEG-GO was also studied. Figure 2**a** illustrates DR Uv spectrum of graphene oxide. The Uv spectra of GO showed absorption bands in the 227-231 nm regions as previously reported for GO because of the π→π* transitions [22]. For PEG-GO, the peak related to GO was observed confirming that GO existed in PEG-GO; in addition, the peak subjected to C–O band for polyethylene glycol was observed at 380-400 nm regions (Figure 2**b**). For the supported catalyst (Because of d→d transitions), the bands for nickel acetat were observed with a shift due to the existence of the supported nickel acetate salts on polyethylene glycol grafted graphene oxide (Figure 2**c**).

In order to study the effect of the modification procedure on the surface morphology, surface FESEM images were prepared, and then they were compared together in Figure 3. As can be seen, the surface morphology was changed by supporting the PEG, leading to the creation of a smoother and more compressed surface than that of unmodified GO. Figure 3**c** illustrates that the surface morphology was changed by supporting the nickel acetate, which led to the disappearance of smoother and compressed surface as compared to that of the unmodified graphene oxide grafted polyethylene glycol.

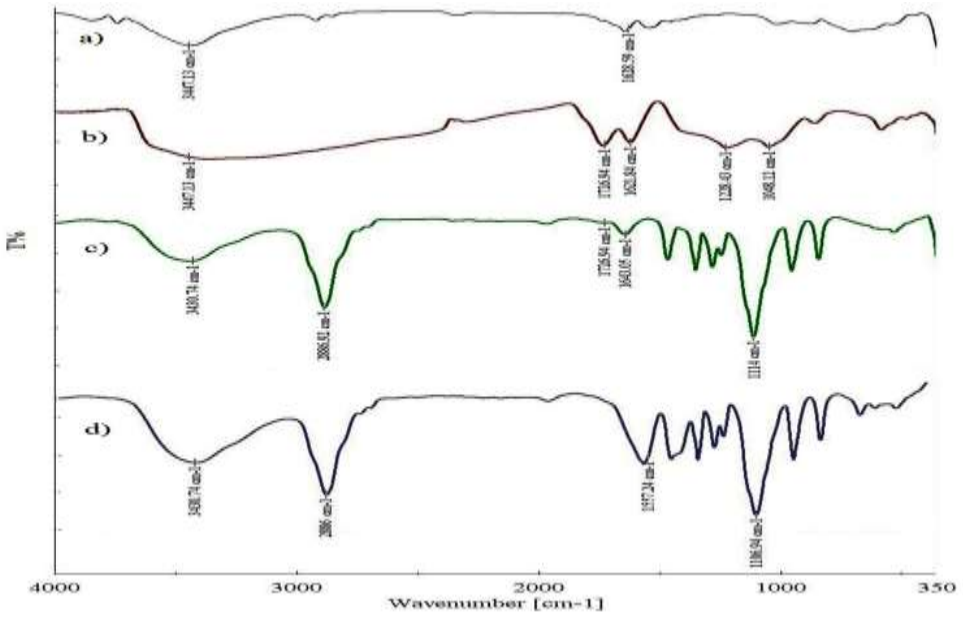

Figure 1. FT-IR spectrum of a) graphite b) GO, c) PEG-GO, d) NiOAC@ PEG-GO

Figure 4 shows XRD patterns of NiOAC, GO, PEG-GO and NiOAC@ PEG-GO. XRD pattern for nickel acetate salt shows a monoclinic structure [24]. The two-theta position of the (001) GO diffraction peak can show a range of ~7-12° two-theta (Cu Kα radiation) depending on the amount of residual

water which is intercalated between basal planes in a GO film. In addition, there is a broad peak at ~19° two-theta because of a disordered component(s) that is/are generated during the chemical processing of graphite in order to make GO [22]. After the modification of GO with PEG, the XRD pattern of GO-PEG showed two characteristic peaks of PEG as previously reported [25] that showed the PEG immobilized on GO. The immobilization of nickel acetate on the surface of GO-PEG resulted in a change in the powder XRD pattern as compared to that for GO-PEG, confirming the formation of a new material and a possible change in interplanar space and crystallinity. From XRD images for the supported catalyst, the caracteristic peaks for the mono-clinic structure of nickel acetate were maintained after immobilization of nickel acetate, and the peaks at 2θ=13.2 and 28.5 for mono-clinic structure of nickel acetate were observed for XRD pattern of the catalyst.

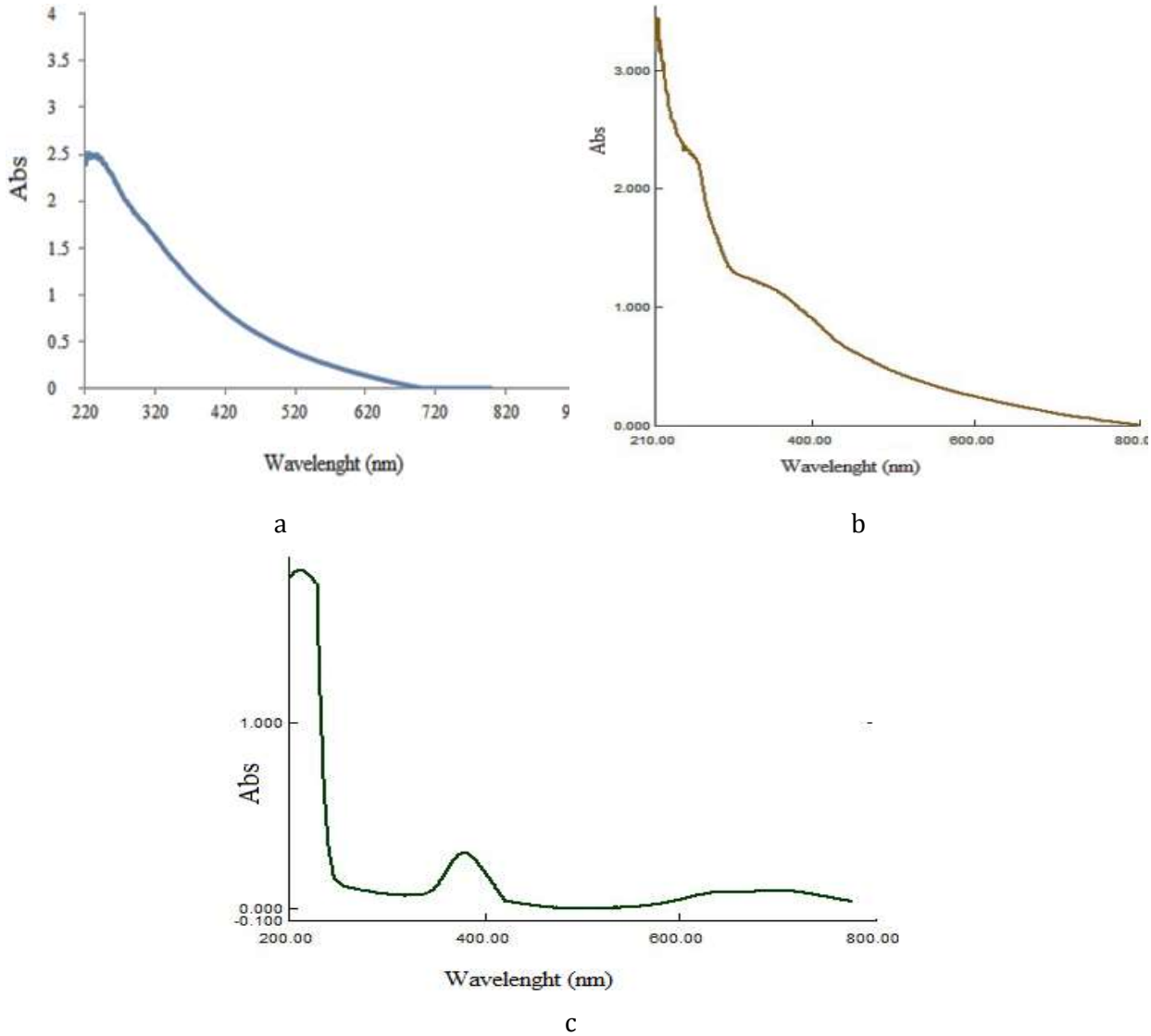

Figure 2. DR Uv-vis spectra of a) GO, b) PEG-GO, c) NiOAC@ PEG-GO

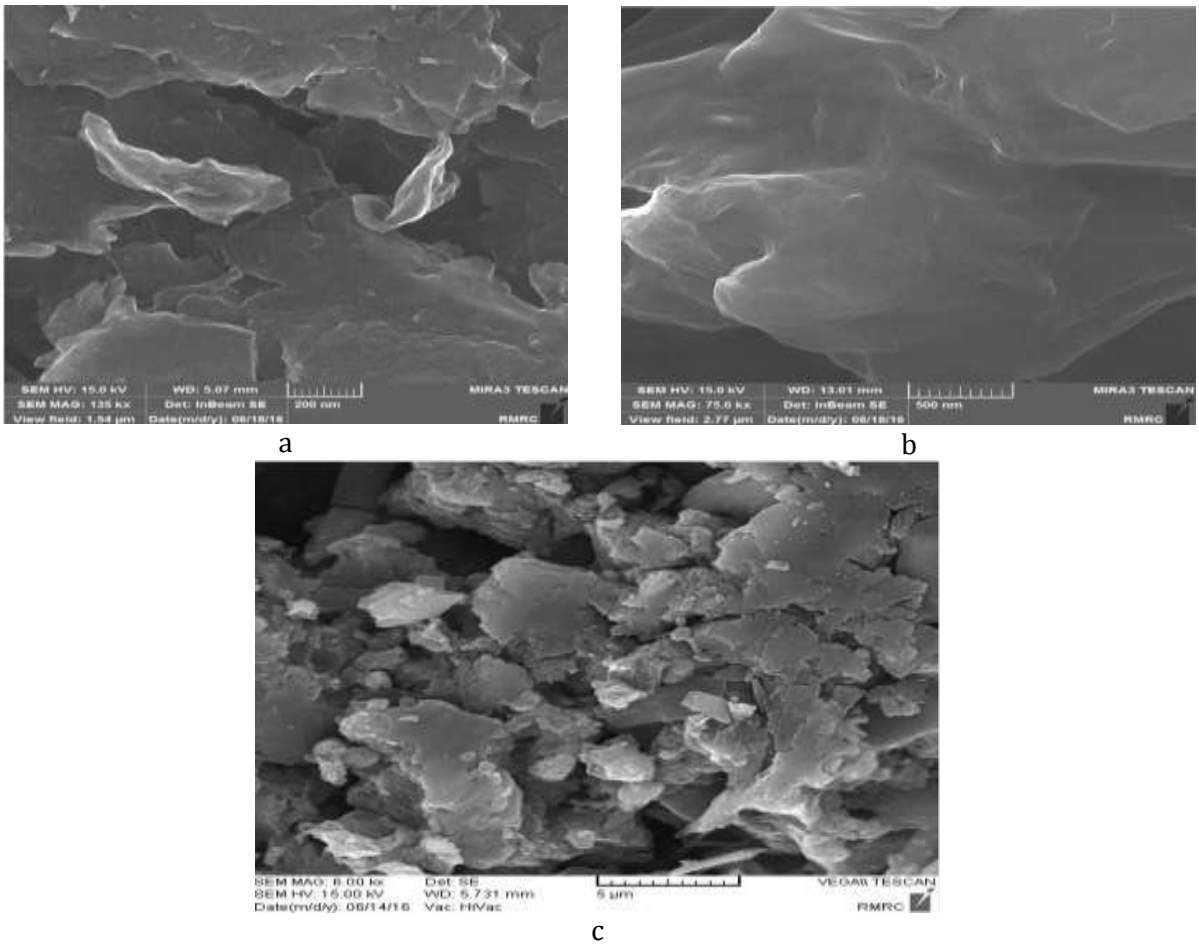

Figure 3. FESEM images of a) GO, b) PEG-GO, c) NiOAC@ PEG-GO

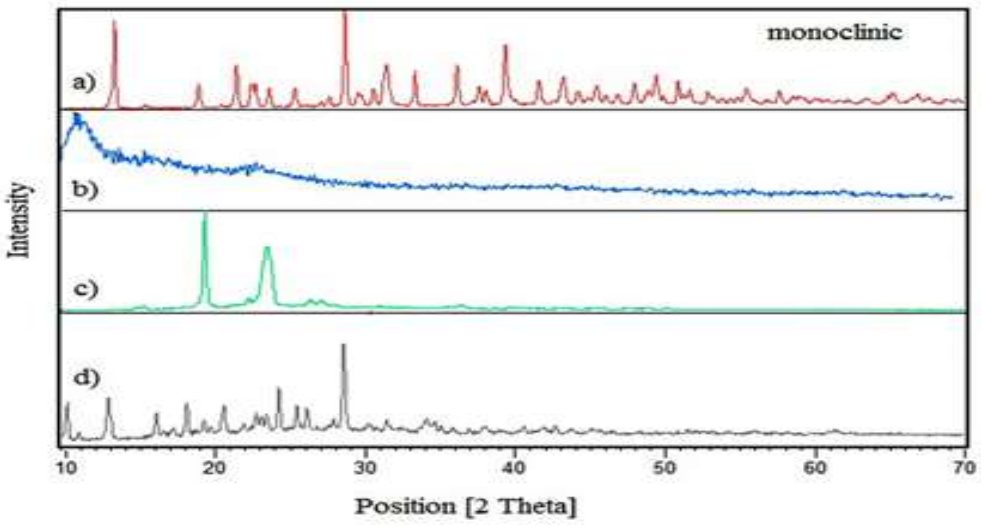

Figure 4. XRD images of a) NiOAC b) GO, c) PEG-GO, d) NiOAC@ PEG-GO

Catalytic activity test

Thioanisole was selected as the model sulfide while using the oxidation procedure. Oxidation of thioanisole was carried out in a flask equipped with a magnetic stirrer and a condanser. In a typical run with a round-bottom flask, 0.5 mL of the solvent was mixed with 0.2 mmol thioanisole. Following the addition of the catalyst and H_2O_2, the reaction was started at the atmospheric pressure and a given set temperature, depending on the test with the reaction time, and then it was recorded. The oxidation procedure was analyzed by the gas chromatography system. To consider the effect of time, catalyst amount and the oxidant amount on oxidation of thioanisole, we examined various conditions based on CCD experiments. Consequently, the results showed that the reaction promoted to obtained sulfone in 99% yield in ethanol at room temperature with oxidant/substrate 3:4.

Statistical analysis and the model fitting

The effect of various factors on the catalytic oxidation of PhSMe was investigated, and the impacts of temperature, oxidant amount and time on the catalytic oxidation of PhSMe, selected as model sulfur compound for optimization, were examined. Design expert 7.0.0 software was used for the regression analysis of the obtained data and in order to estimate the coefficient of the regression equation. The equations were validated by statistical tests, called the ANOVA, to determine the significance of each term in the fitted equations and to estimate the goodness of fit in each case. Response surfaces were drawn for the experimental results as they were obtained from the effect of different variables on the percentage oxidation of PhSMe, in order to determine the individual and cumulative effects of these variables and the mutual interactions between them. The Fisher's F value with a low probability ($p<0.0001$) showed that the model was significant. The multiple correlation coefficient (R^2) demonstrated the goodness of the model. Moreover, R^2 value, 0.985, could be explained by the developed quadratic model, and the predicted R^2 values were in agreement with adjusted R^2, which means that all of terms depicted in the model were significant. In this case, the non-significant lack-of-fit (0.08) confirmed that the quadratic model was valid for this process. In the presented research, the effects of three essential operating parameters including reaction time (A), catalyst amount (B) and oxidant/substrate ratio (C) were systematically evaluated using central composite design procedure. The selected variables are summarized in Table 1.

Comparison between theoretical and experimental data

The CCD equation of actual factors was solved by partial differential calculus for obtaining the optimum value of A, B, C. In this research, the effects of three effective parameters including reaction

time, catalyst amount and O/S ratio were systematically optimized using central composite design software. In this technique, the total number of experimental runs can be calculated by Eq. 1:

$$N = 2n + 2n + nc \quad (1)$$

Where, n and n_c represent the variable number and the replicated number of the central point, respectively. For statistical analyses and optimization of each cycle, a quadratic model was selected as the best model. Design expert (DX7) software was applied for statistical calculations, optimization of the process and determination of the response model. The optimized value is shown below, and Table 2 shows that the optimized data were obtained for this study. A (time) = 31 min, B (catalyst) = 21 mg, C (O/S) = 3.4, for catalyst amount=21 mg. Theoretical R (% oxidation) = 99.4%, and experimental R (% oxidation) were 99% obtained at optimized conditions. The actual obtained conversion based on the optimized condition is shown in Table 2.

The experimental results of CCD showed the significant influence of the selected operating variables. The effect of three process factors including the reaction time, catalyst amount and O/S, as well as interaction between these variables were analyzed by mean of RSM methodology in order to obtain an empirical model as the best response. The final quadratic equation was attained to illustrate the relation among the independent variables and the dependent responses.

Table 1. The range of the independent variables applied in the central composite design

Factor	Name	Units	Type	-Level	+Level	$-\alpha$	$+\alpha$
A	time	min	Numeric	10	30	1.47759	43.5224
B	Cat amount	mg	Numeric	10	35	3.18207	36.8179
C	O/S		Numeric	2	4	1.31821	4.68179

Table 2. Constraints applied for optimization process for oxidation of DBT; catalyst amount: 100 mg

Cat amount	Time (min)	O/S	sufone%
21 mg	31 min	3.4	99

Effect of reaction conditions on conversion of thioanisole using 3D surface diagrams

The combined effect of variables was investigated using 3D surface diagrams. The effect of different levels of oxidant amount and catalyst amount on oxidation of thioanisole, using the nickel acetate supported on modified graphene oxide, can be predicted from the contour plot as shown in

Figure 5. From the contour plot, it can be observed that oxidation percentage increased with oxidant amount and catalyst amount. This could be due to the increase in the exposed surface area of the catalyst. However, it must be noted that after a certain limit, if the amount of oxidant had been increased further, there would have been a saturation point and the conversion would have been decreased because the oxidant would probably have been decomposed. From the results, it was observed that an actual oxidation efficiency of 99% was achieved at O/S ratio 3:4, and 31 min of time. The combined effect of O/S ratio and time on oxidation of thioanisole was shown in the contour plot of Figure 5. The percentage of oxidation was increased with time due to an increase in number of molecules of sulfur compound converted to sulfone. Higher O/S ratio enhanced the peroxo species and increased the oxidation of sulfur compound. From the results, it was observed that a maximal removal efficiency of 99% was achieved at O/S ratio 3:4, and 31 min of time. The combined effect of time and catalyst amount on oxidation of thioanisole was observed in the contour plot of Figure 5. It was shown that % conversion increased with increasing oxidant and time. The maximum conversion of 99% was obtained from catalyst amount 21 mg and time 31 min. As can be seen in Figure 5 **a–f**, overall, the important degree of the tested based on the slope of the 3D surface diagramsson conversion was: O/S ratio>time>catalyst amount.

To establish the general applicability of the process, various sulfides were subjected to the oxidation system using the synthesized catalyst (Table 3, entries 1-12). The reactivities of the sulfur compounds were influenced by two main factors, i.e., the electron density on the S atom and the steric hindrance of the sulfur compound.

Catalytic behavior, separation, and recyclability

Various oxidants were used for the oxidation of thioanisole, and the results showed that maximum conversion was achieved with hydrogen proxide (Figure 6).

For each of the repeated reactions, the catalyst was recovered, washed thoroughly with ethanol and dried before being used with fresh thioanisole and hydrogen peroxide. Then, the catalysts were consecutively reused four times. FT-IR spectrum of the catalyst after reused was taken, and the result showed the peaks corresponding to PEG shifted to lower vibrational band from 1114 cm^{-1} to 1105.95 cm^{-1} and the peak related to acetate group was shown at 1500-1596 cm^{-1} ranges (Figure 7).

In using hydrogen peroxide as an environmentally benign and terminal oxidant, it was found that, as shown in Table 4, using synthesized catalyst could result in a good yield (Entry 4), but using NiOAC, GO, PEG-GO alone showed nearly trace catalytic activity (Entry 1-3). The stability of the supported catalyst was monitored using multiple sequential oxidation of thioanisole with hydrogen peroxide under magnetic stirring.

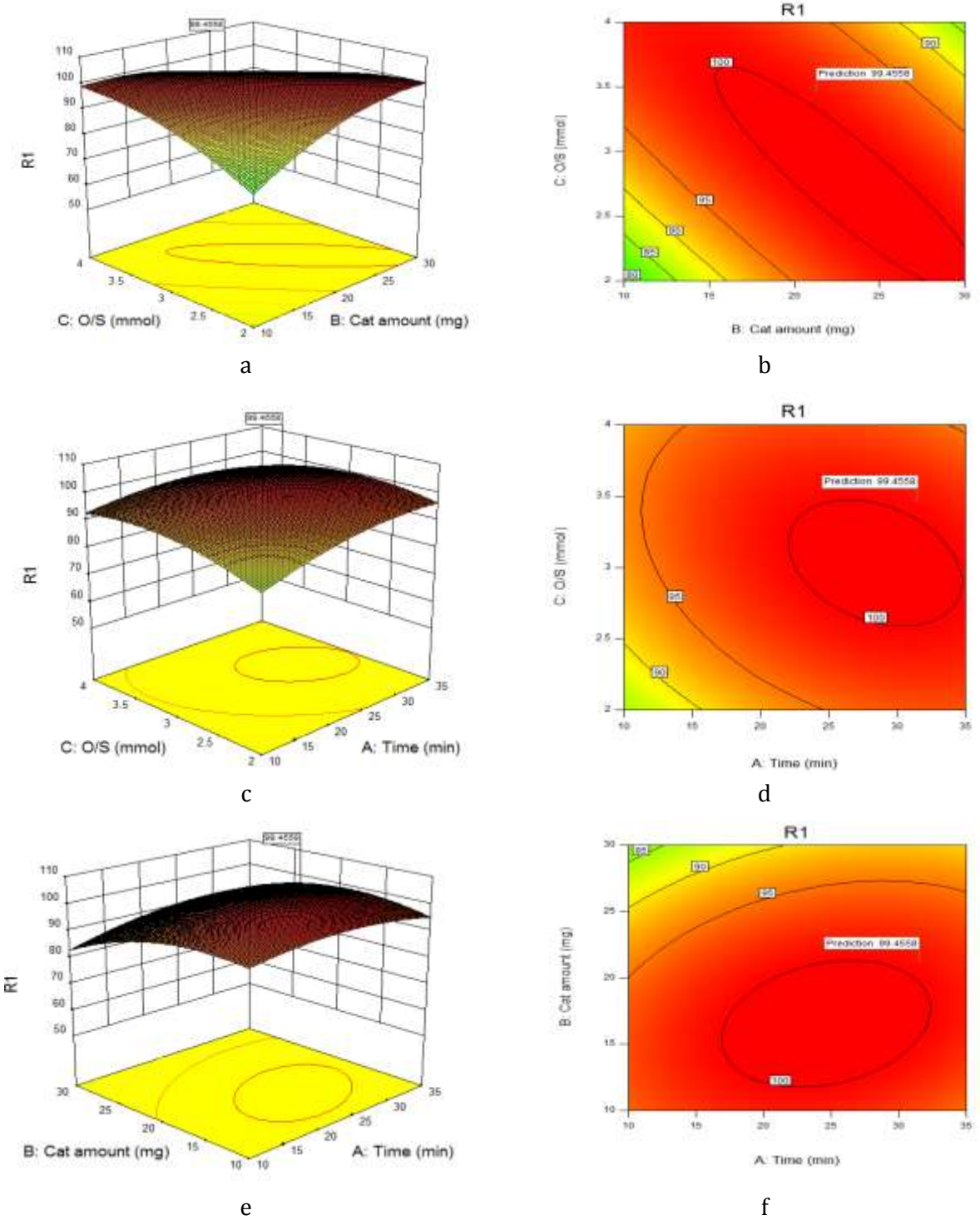

Figure 5. Three dimensional response surface graph and counter plots for the oxidation of PhSMe, % sulfone versus catalyast amount and O/S, counter plots for catalyast amount and O/S, % sulfone versus time and O/S, counter plots for time and O/S, % sulfone versus catalyast amount and time, counter plots for time and catalyat amount, temperature 25 °C, ethanol as green solvent

Table 3. Oxidation of sulfides to sulfone product with H_2O_2 catalyzed by synthesized catalyst. GC yields based on the toluene as the internal standard

Entry	Sulfur compound	Time (min)	Yield (%)
1	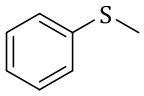	31	99-100
2	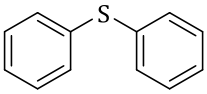	30	85-92
3	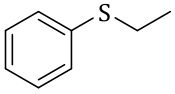	30	92
4	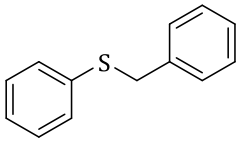	20	84-89
5	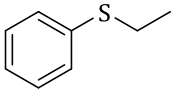	25	92-95
6	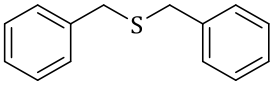	20	91-96
7	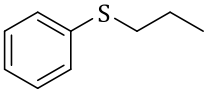	15	83-86
8	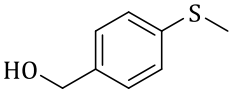	40	95-98
9	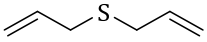	25	89-92
10	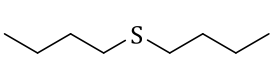	25	93-96
11	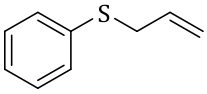	30	95-98
12	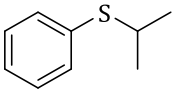	25	82-88

Figure 6. Effect of oxidant nature on oxidation of thioanisole to sulfone under optimized conditions

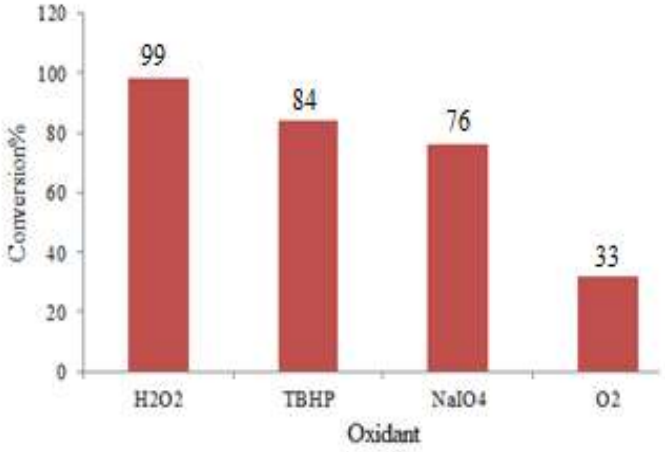

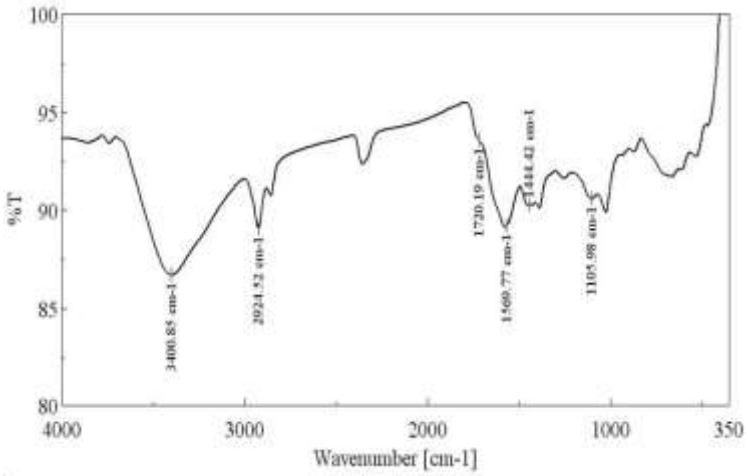

Figure 7. FT-IR spectrum of supported catalyst after reused from oxidation of methyl phenyl sulfide with H_2O_2 catalyzed by catalyst

Table 4. Oxidation of thioanisole to sulfone products using different catalysts at room temperature under optimized conditions, Conversion determined by GC

Entry	Catalysts	Conversion% (Sulfoxide)
1	NiOAC	40%
2	GO	trace
3	PEG-GO	trace
4	NiOAC@ PEG-GO	99%

Table 5 compares the catalytic activity of the supported catalyst with those of other reported catalysts for the oxidation of sulfides. There are no reports about catalytic oxidation of thioanisole by the catalyst synthesized in this work.

The proposed mechanism is shown in Scheme 4; the immobilized nickel acetate reacted with H_2O_2 to generate peroxo species. This species facilitated the transfer of the electrophilic oxygen to the sulfide, yielding the corresponding sulfone. The sulfone product could be easily removed by extraction.

Conclusion

NiOAC-functionalized graphene oxide (NiOAC@ PEG-GO) was prepared by anchoring NiOAC on the surfaces of nanoparticles of GO coated with PEG. The catalysts were used in the oxidation of thioanisole and were selectively oxidized to their corresponding sulfone under various reaction conditions successfully. The NiOAC@ PEG-GO catalyst also showed a good catalytic activity for the oxidation procedure using H_2O_2 as the oxidant.

Table 5. Comparison of reaction data for the present method and other reported methods

Catalyst	Oxidation of sulfides	Ref.
Three dimension GO (3D)	Thioanisole	44
GO	Sulfide	45
GO@Co–Cu–Zn doped by Fe_3O_4 / Co_3O_4-MoO_3	Sulfides/H_2O_2	46

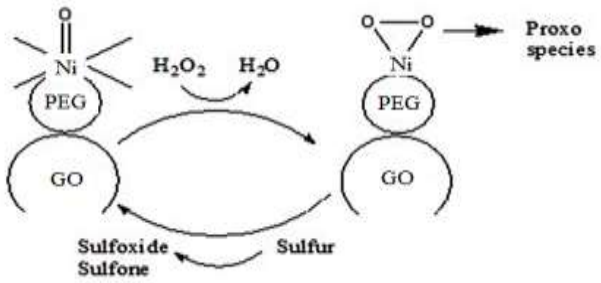

Scheme 4. Proposed mechanism for oxidation of sulfide with NiOAC@ PEG-GO catalyzed by H_2O_2

Disclosure statement

No potential conflict of interest was reported by the authors.

References

[1]. Stankovich S., Dikin D.A., Dommett G.H.B., Kohlhaas K.M., Zimney E.J., Stach E.A., Piner R., Nguyen S.T., Ruoff R.S. *Nature*, 2006, **442**:282

[2]. Geim A.K., Novoselov K.S. *Nature Mater.*, 2007, **6**:183

[3]. Brodie B.C. *Philosophical Transactions of the Royal Society of London*, 1859, **149**:249

[4]. Marcano D.C., Kosynkin D.V., Berlin J.M., Sinitskii A., Sun Z., Slesarev A., Alemany L.B., Lu W., Tour J.M. *ACS Nano*, 2010, **4**:4806

[5]. Stankovich S., Dikin D.A., Piner R.D., Kohlhaas K.A., Kleinhammes A., Jia Y., Ruoff R.S. *Carbon*, 2007, **4***:*1558

[6]. Zhu Y., Murali S., Cai W., Li X., Suk J.W., Potts J.R., Ruoff R.S. *Advanced materials*, 2010, **22**:3906

[7]. Hajjar Z., Kazemeini M., Rashidi A., Bazmi,M. *Catalysis Letter*., 2015, **145**:1660

[8]. Mabayoje O., Seredych M., Bandosz T.J. *ACS Appl. Mater. Interfaces*., 2012, **4**:3316

[9]. Eda G., Fanchini G., Chhowalla M. *Nature nanotechnology*, 2008, **3**:270

[10]. Stankovich S., Piner R.D., Nguyen S.T., Ruoff R.S. *Carbon*, 2006, **44**:3342

[11]. Khaled M. *Res. Chem. Intermedia*., 2015, **41**:9817

[12]. Sun B., Yu X., Wang L., Feng L.J., Li C.H. *J. Fuel Chem. Technol*., 2016, **44**:1074

[13]. Menzel R., Iruretagoyena D., Wang Y., Bawaked S.M., Mokhtar M., Al-Thabaiti S.A., Basahel S.N., Shaffer M.S.P. *Fuel*, 2016, **181**:531

[14]. Li S., Mominou N., Wang Z., Liu L., Wang L. *Energy Fuels*, 2016, **30**:962

[15]. Totten G.E., Clinton N.A. *J. Macromolecul. Sci*., Part C, 1998, **38**:77

[16]. Toke L., Szabo G.T. Poly (ethylene glycol) chemistry: biotechnical and biomedical applications, 1977, **93**:421

[17]. Sawhney A.S., Pathak C.P., Hubbell J.A. *Macromolecules*, 1993, **26**:581

[18]. Van Truong N.G., Norris A.R., Shin H.S., Buncel E., Bannard R.A.B., Purdon J.G. *Inorg. Chim. Acta,* 1991, **184**:59

[19]. Neumann R., Sasson Y. *J. Molecul. Catalysis*, 1985, **31**:81

[20]. Neumann R., Dermeik S., Sasson Y. *Israel J. Chem*., 1985, **26**:239

[21]. Pleșa I., Noțingher P.V., Schlögl S., Sumereder C., Muhr M. *Polym*, 2016, **8**:173

[22]. Marcano D.C., Kosynkin D.V., Berlin J.M., Sinitskii A., Sun Z., Slesarev A., Alemany L.B., Lu W., Tour J.M. *ACS Nano*., 2010, **4**:4806

[23]. Mansourpanah Y., Shahebrahimi H., Kolvari E. *Chem. Eng. Res. Design*, 2015, **104**:530

[24]. Hanawalt, *Anal. Chem.*, 1938, **10**:475

[25]. Tan B., Huang Z., Yin Z., Min X., Liu Y.G., Wu X., Fang M. *RSC Adv*., 2016, **6**:15821

How to cite this manuscript: Mehrnaz Alem, Shahnaz Kazemi*, Abbas Teimouri*, Hossein Salavati. Green oxidation reactions by graphene oxide-based catalyst with aqueous hydrogen peroxide. *Asian Journal of Green Chemistry*, 3(3) 2019, 366-381, DOI: 10.22034/ajgc.2018.144166.1097